Lawrence Berkeley National Laboratory
Recent Work

Title
Assessment of Specimen Noise in HREM Images of Simple Structures

Permalink
https://escholarship.org/uc/item/0w45135w

Journal
Ultramicroscopy, 50

Authors
Paciornik, S.
Kilaas, R.
Dahmen, U.

Publication Date
1993-02-16

eScholarship.org Powered by the California Digital Library
University of California

LBL-33720
UC-404
Preprint

Lawrence Berkeley Laboratory

UNIVERSITY OF CALIFORNIA

Materials Sciences Division

National Center for Electron Microscopy

Submitted to Ultramicroscopy

Assessment of Specimen Noise in HREM Images of Simple Structures

S. Paciornik, R. Kilaas, and U. Dahmen

February 1993

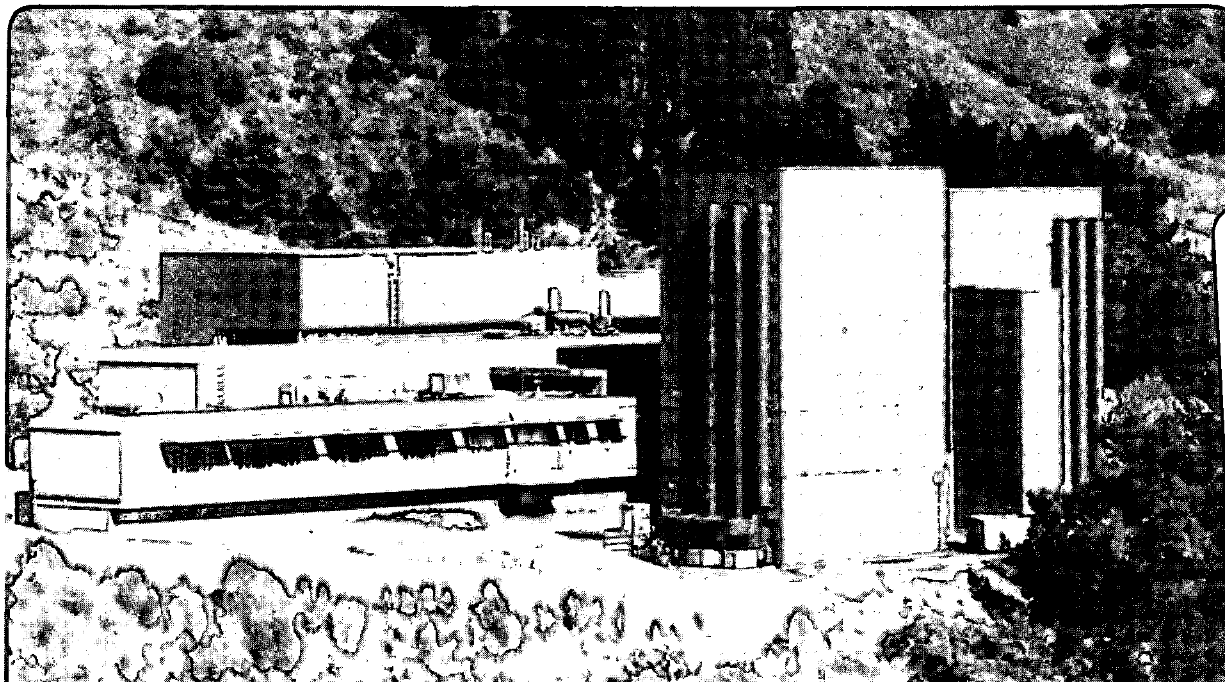

REFERENCE COPY
Does Not
Circulate
Bldg. 50 Library.
LBL-33720
Copy 1

Prepared for the U.S. Department of Energy under Contract Number DE-AC03-76SF00098

DISCLAIMER

This document was prepared as an account of work sponsored by the United States Government. While this document is believed to contain correct information, neither the United States Government nor any agency thereof, nor the Regents of the University of California, nor any of their employees, makes any warranty, express or implied, or assumes any legal responsibility for the accuracy, completeness, or usefulness of any information, apparatus, product, or process disclosed, or represents that its use would not infringe privately owned rights. Reference herein to any specific commercial product, process, or service by its trade name, trademark, manufacturer, or otherwise, does not necessarily constitute or imply its endorsement, recommendation, or favoring by the United States Government or any agency thereof, or the Regents of the University of California. The views and opinions of authors expressed herein do not necessarily state or reflect those of the United States Government or any agency thereof or the Regents of the University of California.

LBL-33720

Assessment of Specimen Noise in HREM Images of Simple Structures

S. Paciornik*, R. Kilaas, & U. Dahmen

Materials Science Division
National Center for Electron Microscopy
Lawrence Berkeley Laboratory
University of California, Berkeley, CA 94720

*on leave from DCMM, PUC-Rio de Janeiro
P.O. Box 38008
22452, Rio de Janeiro, Brazil

Ultramicroscopy, submitted

This work was supported in part by the Director, Office of Energy Research, Office of Basic Energy Sciences, Materials Sciences Division of the U.S. Department of Energy under Contract No. DE-AC03-76SF00098.

ASSESSMENT OF SPECIMEN NOISE IN HREM IMAGES OF SIMPLE STRUCTURES

S. Paciornik*, R. Kilaas and U. Dahmen
National Center for Electron Microscopy, MSD, Lawrence Berkeley Laboratory,
University of California, Berkeley, Ca. 94720

* on leave from DCMM, PUC-Rio, P.O.Box 38008, 22452, Rio de Janeiro, RJ Brazil

ABSTRACT

Displacements of image spots representing atomic columns in a high resolution image may be due either to displacements of atomic columns or to specimen noise. The effect of specimen noise on the accuracy with which an atomic column can be located is assessed by evaluating the root mean square deviation of the intensity center of mass of image dots. Optimized methods for experimental assessment of this effect are developed and applied to simulated and experimental images.

INTRODUCTION

High resolution electron microscopy (HREM) is a primary tool for studying the atomic structure of defects in crystals. However, the quantitative analysis of defect structures is seriously limited by specimen noise due to contamination or oxide layers on the surfaces of a thin foil. Interpretation of HREM is usually aimed at extracting two parameters; composition and location of atomic columns in a zone axis orientation. If both could be extracted independently it would be possible to determine atomic structure completely and accurately from HREM images obtained in a few different zone axis

orientations. However, this method of structure determination is still in its infancy due to limitations in microscope resolution and the restrictions of specimen noise.

High resolution images consist of characteristic patterns of intensity. These patterns depend upon the atomic structure and the imaging conditions (i.e., defocus, thickness, microscope parameters, etc.). Analysis of such images is usually performed by comparing experimentally obtained images with images simulated from different models. The best fit is normally determined visually, although more quantitative methods of comparison and refinement have been employed for perfect crystals [1] and more recently for defects [2].

For complex crystal structures the effects of atom location and composition are intertwined such that small atomic displacements may have a similar effect on the image as a variation in composition, and the two effects are not easily separated. However, for simple monatomic structures such as fcc or bcc metals observed in directions where the structure projects into well-separated atomic columns, image interpretation is greatly simplified: under weak phase object, Scherzer imaging conditions, each atomic column is imaged as a black dot. Variations in intensity and position of individual image dots can be due to variations in composition or location of atomic columns. Unfortunately, both effects may also arise from random noise superimposed on the periodic image due to an amorphous oxide or contamination film on the surfaces of the thin foil. To extract quantitative information about atomic structure or composition from HREM micrographs, even for simple structures, it is therefore necessary to assess carefully the effect of specimen noise.

Gibson has evaluated the effect of noise on the detectability of composition variations in high resolution images of Si [3]. He defined a signal to noise ratio by comparing the intensities of the full image with an image of the noise in the same frequency as the main Bragg reflections. The latter image was obtained by appropriate Fourier filtering. He distinguished between shot noise (present in the image of the hole near the

thin edge of a foil) and specimen noise (due to contamination or oxide layers on the sample surfaces). In all cases, specimen noise was by far the more limiting factor, with ion milling producing the highest and UHV-treatment the least amount of specimen noise.

More recently, the problem of compositional sensitivity in high resolution images of compound semiconductors has been addressed by Ourmazd et al. [4]. A signal to noise ratio was defined by a "vector pattern recognition technique", essentially the cross correlation coefficient between each individual unit cell in the image and that of an average unit cell obtained from the same image. Specimen noise is found as the deviation of cross correlation coefficients from unity. When imaging and foil preparation conditions are optimized, this technique of "chemical lattice imaging" can achieve signal to noise ratios of 9 for $GaAs/Al_{0.4}Ga_{0.6}As$ superlattice structures. The same technique has also been applied to the detection of compositional variations in NiAl superalloys [5]. However, due to the smaller lattice spacings and the higher contribution of specimen noise from the electrochemical thinning technique, signal to noise ratios between NiAl and NiNb were as low as 3.

Notice that in both of the evaluations of specimen noise described above the objective is to determine *composition*. The underlying assumption is that the locations of the atomic columns are fixed on a periodic lattice. The converse problem, that of determining local variations in the *location* of atomic columns whose composition is constant, is encountered in the case of structural defects. It is well-known that even though the Scherzer resolution limit may only be 1.6Å, HREM allows the localization of structural features to within a fraction of an Ångstrom [6]. However, this accuracy is also compromised by specimen noise. For example, image simulations have shown that a layer of amorphous oxide (random noise) on the surfaces of a thin foil of perfect crystalline Si can lead to significant shifts in image intensities and centroid positions for individual atomic columns [7].

Often, the effect of specimen noise is reduced by averaging over a number of similar image features. For example, in periodic grain boundaries, low noise images can be obtained by averaging over a number of repeat units [e.g.8]. However, this procedure sacrifices spatial resolution, one of the principal advantages of HREM. In the same manner, rigid body shifts at grain boundaries can be measured with high accuracy because they compare the relative positions of whole blocks or rows of atoms. Any random noise is thus effectively reduced to insignificant levels. Thus, the rigid body shift parallel to a grain boundary can be measured to within 0.1 Å [6] while the shift normal to a grain boundary has been measured with an accuracy of 0.04 Å [9]. It has been pointed out, however, that such measurements are very sensitive to slight instrument and sample misalignments and must be interpreted with caution [10].

Displacement fields around lattice defects such as dislocations or ledges in interfaces have been measured by comparing experimental images with overlaid models. The displacements are then easily seen as the deviation of individual image dots from the overlaid reference lattice [11]. An effective alternative technique for visualizing and measuring displacement fields from HREM images is based on the moiré effect between an image and an undistorted reference image of similar magnification [12]. The effect of specimen noise in this type of measurement is a blurring of the moiré pattern. This technique has also been employed to identify multilayer structures when a change in composition is visible as a small change in lattice spacing [13].

Notice that all of these measurements are based on the assumption that the image dot faithfully represents the location of an atomic column. Fourier imaging theory shows that this is indeed the case for sufficiently small and sufficiently delocalized displacements. Only large, highly localized displacements such as those at the core of a dislocation will not always be imaged faithfully [14] . However, even in the core of a dislocation or a structural unit in a grain boundary, a minimum interatomic distance will be maintained. For projections of widely spaced atomic columns the projected mean interatomic spacing is

similar to the minimum interatomic spacing. This limits both the magnitude and the localization of the displacements, and it can be shown that under Scherzer imaging conditions all physically reasonable displacements of atomic columns are imaged faithfully. In the absence of specimen noise the intensity center of mass of image dots is therefore a direct representation of the location of atomic columns.

However, specimen noise inherent in all non-averaged, unfiltered HREM images can severely limit the accuracy with which an image dot represents an atomic column. For a quantitative structural analysis of defects it is therefore essential to assess the contribution of specimen noise to an experimental image. The present paper describes an optimized procedure for noise assessment using both simulated and digitized experimental images.

DESCRIPTION OF THE METHOD

To assess displacements of image intensity peaks due to contamination or oxide layers, it is necessary to extract the image peak positions and compare them with a set of reference peak positions. Thus the method depends on obtaining the following two lists of positions:

- a list obtained by finding the center of mass of intensity peaks located near atomic positions in the experimental image.
- a second list created by performing a least-squares fit of a 2D lattice upon the positions of the first list. This list will locate to a good approximation the positions of intensity peaks in the absence of noise.

Once both lists are obtained the root mean square (rms) deviation between the lists is calculated and used as a direct measure of the noise in the image.

The peak-finding is a critical step in the process. The routine first finds an initial peak with the precision of a single pixel and proceeds to locate an intensity center of mass to sub-pixel accuracy using the pixel intensity values in a circular region around the initial

peak. The choice of radius for the center of mass calculation is determined by the extent of the peaks and their separation. While the radius should be chosen large enough to ensure high accuracy in the determination of the center of mass, it cannot be chosen larger than the half-spacing between peaks, in which case, neighboring peaks will influence the location of the center of mass.

Although the peak-finding routine in general has no difficulty finding peaks in simulated images, even in those that are quite noisy, problems are frequently encountered in the case of experimental images. Mainly due to the presence of shot noise, the employed peak-finding routine often finds spurious maxima which are not localized near atomic positions. This causes difficulties in applying the peak-finding routine directly to the experimental images. The influence of shot noise can be reduced by applying a real space convolution filter to the experimental images prior to peak finding. In order to preserve the symmetry of the original intensity peaks, the kernel of the filter should have circular symmetry and the kernel used in this work simulated a circular gaussian function. This is equivalent to the use of a low pass gaussian filter in frequency space where the half-width of the low-pass filter is inversely proportional to the size of the gaussian in real space. As the gaussian kernel increases in real space, more high frequencies are filtered out.

Unfortunately, the filtering procedure also reduces the noise which one is interested in measuring. In order to reduce the bias to the resulting noise measurements, the gaussian filter should be constructed with the smallest possible kernel. A kernel with 1 pixel standard deviation proved to be sufficient in the vast majority of situations.

Once the peak positions are reliably located, the next step is the least-squares lattice fitting. This routine takes as input the original peak list and initial estimates for the lattice vectors $\vec{u}$ and $\vec{v}$. These values are obtained from average distances between selected peaks in both unit directions. The lattice fitting then iterates these values and returns best estimates in a least-squares sense, together with a fitted peak list and the rms deviation between the

original peak list and the fitted peak list. This value can be used as a direct measurement of the error associated with localizing atomic positions.

RESULTS

Simulated Images

In order to test the method, simulated images of two different multi-layer structures (A and B) were created using NCEMSS (National Center for Electron Microscopy Simulation Software[15]. Both structures were composed of seven different layers of amorphous material, each 4Å thick, on top of a 20Å fcc crystal layer with lattice parameters of 3.6 and 5Å for structures A and B respectively. The various amorphous layers were obtained from different sections of amorphous material created by placing atoms in a "box" in random positions, taking care that no atoms were placed closer than twice the atomic radius.

Eight simulated images (256 x 256 pixels, 256 gray shades) were calculated, under Scherzer condition, for each structure corresponding to a 20Å layer of crystalline material with zero to 7 layers of amorphous material. The two sets of eight images are shown in figures 1a and 1b for structures A and B respectively.

The method described above was applied for each image in the two series of simulated images, using the SEMPER[16] software for finding peak positions and for lattice fitting. The rms values of displacement of peak positions from fitted lattice sites for each series of images, plotted as a function of the ratio of amorphous to crystalline layer thickness, are shown in Figure 2. As can be seen from this figure, there is a direct relationship between the amorphous layer thickness and the rms deviation. This result validates the use of the rms value as a direct assessment of atomic positioning error.

It should be noted that although the origin of the noise is contamination or oxide layer, the relevant information for image analysis is not the layer thickness but the rms deviation because that is the factor that limits the accuracy of structure determination.

Experimental Images

In order to test the method under more realistic conditions a micrograph of a wedge shaped platinum foil was digitized and the same procedure applied. A field of 2048 by 2048 pixels is shown in figure 3. The amorphous layer is clearly visible and the ratio of amorphous to crystalline material decreases as we move away from the border.

Four different 512 by 512 pixel windows were chosen in different regions of the image corresponding to different average ratio of amorphous to crystalline material. The windows are shown superimposed on Figure 3. Peak lists were generated from both unprocessed images and images processed by applying a low pass gaussian filter. It should be noted that without the use of a low pass filter prior to peak finding, several spurious peaks were found by the peak finding routine. The calculated rms deviation for each of the four windows, both filtered and unfiltered are listed in Table 1.

The results show a well behaved relationship between increasing ratio of amorphous to crystalline material and rms deviation. As previously mentioned, the filtering procedure reduces noise. This is accurately reflected in the lower values for the rms deviation in the processed images.

The rms deviation obtained for each window is an average value for the region considered. By reducing the size of the windows, the variation in the ratio of amorphous to crystalline material can be sampled at smaller intervals. However, when the window becomes too small, the accuracy in the fitted lattice decreases, since the number of peaks enclosed by the window is too small to give good statistical values for the lattice parameters. It should be noted that in this regime the value of the rms deviation should

decrease because the fitting *precision* increases when the number of lattice sites decreases although that does not represent a more *accurate* fit for the whole sample.

In order to determine an optimum size for the window the rms deviation was obtained for different sized windows centered on the same position as window 1. A plot of resulting values against the number of atoms inside each window is shown in figure 4.

Three characteristic features are apparent.

First, as the number of atoms decreases past a certain minimum number, the rms tends to zero as the lattice fitting becomes trivial.

Secondly, oscillations in the rms deviation can be observed for a certain regime of window size. This arises from problems associated with intensity peaks located near the borders of the window. As the window increases in size, it will cut through intensity peaks at random, biasing the center of mass calculation, and the contribution of the border peaks will cause the rms deviation to fluctuate. The amplitude of this fluctuation decreases as the window size increases because the ratio of border atoms to internal atoms also decreases. Based on the specific peak-finding algorithm used it is possible to show that this fluctuations are always positive. Thus any rms value obtained from this graph is at most an upper bound to the real rms deviation.

Finally, as the window increases the rms deviation approaches its true value. Although not shown, the same features were observed when using simulated instead of experimental images.

Thus from fig. 4, the minimum number of atoms (window size) required to determine the rms deviation is about 100. Larger windows will result in more accurate statistics but in wedge-shaped foils this may result in systematic errors by averaging over areas with varying thickness and hence signal to noise ratio.

SUMMARY

The accuracy with which atomic columns can be located from high resolution images of simple monatomic structures has been assessed. It was found that the most important limitation is due to random noise arising from contamination or oxide layers on the specimen surfaces. This specimen noise has been characterized by its effect on the location of image spots via the root mean square deviation from an average lattice. Under typical experimental conditions the root mean square deviation of image spots is in the order of 0.2Å. For a good experimental assessment of the noise level it is necessary to sample an area containing about 300 atomic columns. Larger areas do not improve the statistics but increase possible systematic errors due to local variations in the relative thicknesses of crystalline foil and amorphous surface layers.

Specimen noise represents an inherent limitation to the accuracy of structure determination at defects such as grain boundaries. To determine atomic positions with an accuracy better than this inherent limit it is necessary to improve signal to noise levels, either by physically reducing the level of specimen noise or by averaging over several repeat units. The first approach requires major improvements in sample preparation and microscope vacuum, the second sacrifices spatial resolution and presents difficulties for non-periodic defects. To determine the number of repeat units necessary for a desired accuracy of atomic column location is a matter of standard statistical methods.

The present work is a first step in establishing the possibilities and limitations of direct structure determination from high resolution images of defects in simple monatomic structures. Application of the procedures developed here to the determination of the atomic structure of grain boundaries in Al is currently underway.

ACKNOWLEDGMENTS

This work is supported by the Director, Office of Energy Research, Office of Basic Energy Sciences, Materials Sciences Division of the U.S. Department of Energy under Contract No. DE-ACO3-76SFOOO98. One of the authors (S.P.) acknowledges the support from Conselho Nacional de Desenvolvimento Científico e Tecnológico - CNPq, Brazil.

REFERENCES

1. A.R. Smith and L. Eyring, Ultramicroscopy 8, 65 (1982).
2. W.E. King and B.S. Lawver, "Refinement of Interface Atomic Structures from HREM Images", in press.
3. J.M. Gibson and M.L. McDonald, Mat. Res. Soc. Symp. Proc. Vol. 82, 109 (1987)
4. A. Ourmazd, F.H. Baumann, M. Bode and Y. Kim, Ultramicroscopy 34, 237 (1990).
5. J.M. Pénisson, M. Bode, F.H. Baumann and A. Ourmazd, Phil. Mag. Lett. 64, 269 (1991).
6. A. Bourret, MRS Proc. 138, 3 (1989).
7. R. Kilaas and R. Gronsky, Ultramicroscopy 16, 193 (1985).
8. U. Dahmen, C.J.D. Hetherington, M.A. O'Keefe, K.H. Westmacott, M.J. Mills, M.S. Daw and V. Vitek Phil Mag. Lett., 62, 327 (1990).
9. G.J. Wood, W.M. Stobbs and D.J. Smith, Phil Mag. A 50, 375 (1984).
10. R. Hull, Y.F. Hsieh, K.T. Short, A.E. White and D. Cherns, MRS Proc. 183, 91 (1990).
11. J.M. Pénisson, R. Bonnet, R. Loubradou and C. Derder, MRS Proc. 238, 412 (1992).
12. C.J.D. Hetherington and U. Dahmen, Proc. Pfefferkorn conf. (1992), in press.

13. R. Bierwolf, M. Hohenstein, P. Phillipp, O. Brandt, G.E. Crook and K. Ploog, Ultramicroscopy, in press.
14. M. Mills, private communication.
15. R.Kilaas, Proc. 22nd Annual Conference of the Microbeam Analysis Society, 293 (1987).
16. W.O Saxton, T.J. Pilt and M. Horner; Ultramicroscopy 4, 343 (1979).

	rms deviation (Å)	
Window #	Unfiltered	Filtered
1	0.22	0.18
2	0.23	0.20
3	0.25	0.21
4	0.30	0.25

Table 1
Rms deviation for the unfiltered and filtered windows shown in figure 3

Fig. 1 - Two sets of simulated images of crystalline material with varying amorphous surface layer thickness fraction, showing the effect of amorphous contamination on apparent atom positions. In each set, the number of amorphous layers increases from zero in the top left image to seven in the bottom right image. (a) Structure A - lattice parameter 3.6Å and (b) Structure B - lattice parameter 5Å.

Figure 2.- Rms deviation versus amorphous to crystal thickness ratio. (a) Structure A and (b) Structure B

Figure 3. HRTEM image of a wedge shaped Pt foil showing the four windows used to measure rms deviation for different average amorphous noise levels.

Figure 4. Rms deviation as a function of the number of atoms inside the measurement window (see text). Figure 4b is an enlarged view of a portion of figure 4a showing the behavior of the rms deviation as the number of atoms approaches zero.

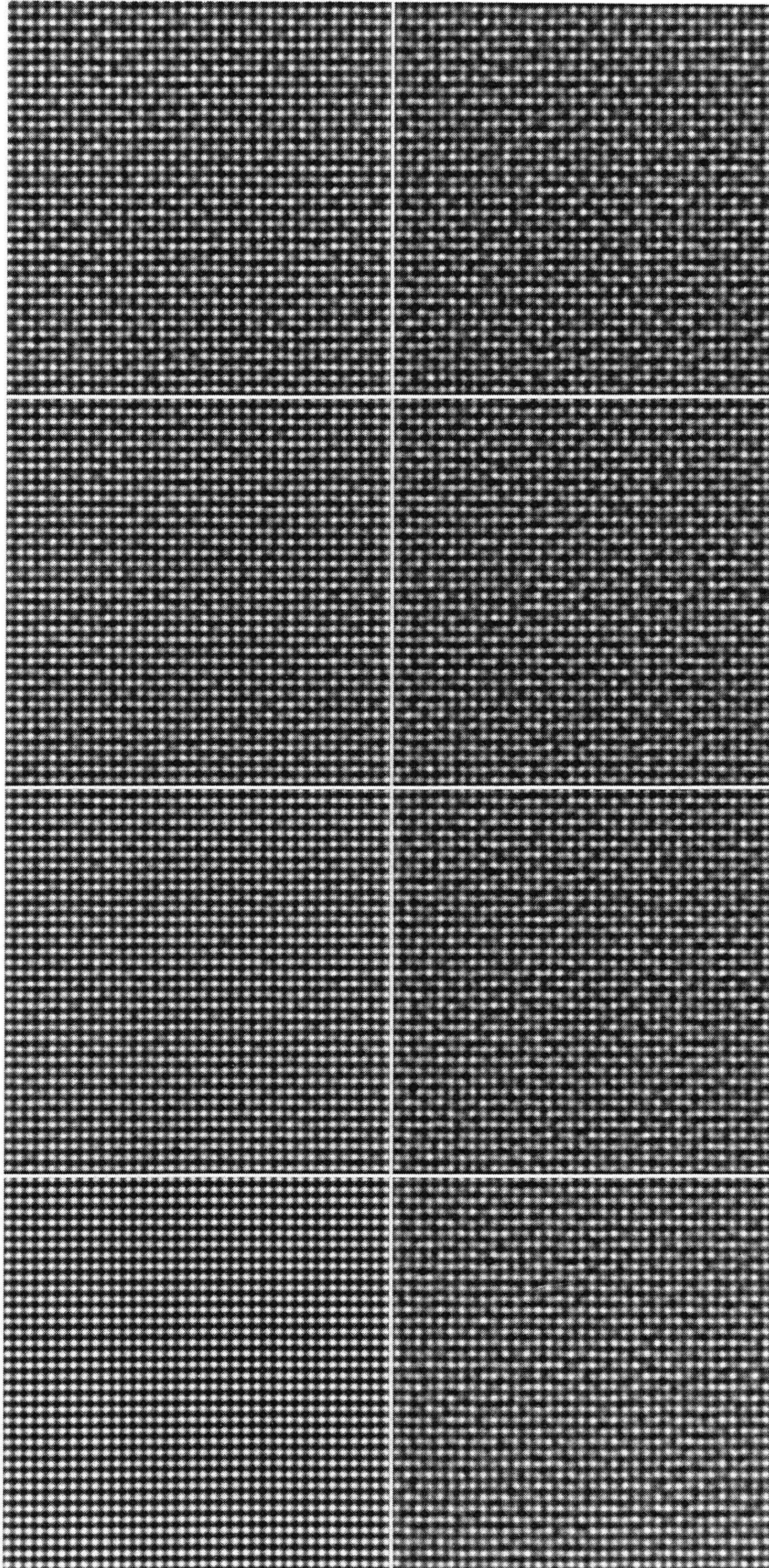

Figure 1a

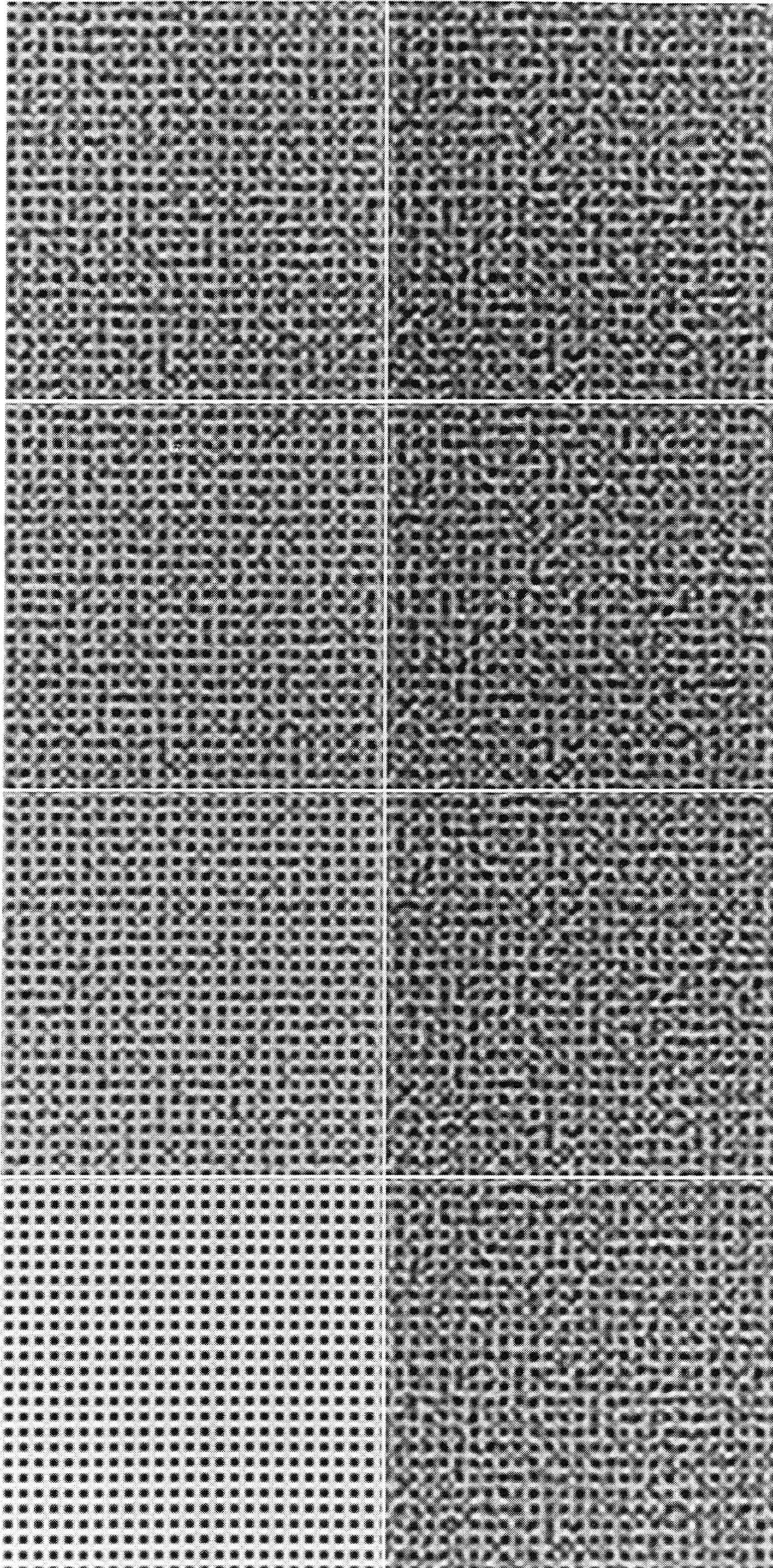

Figure 1b

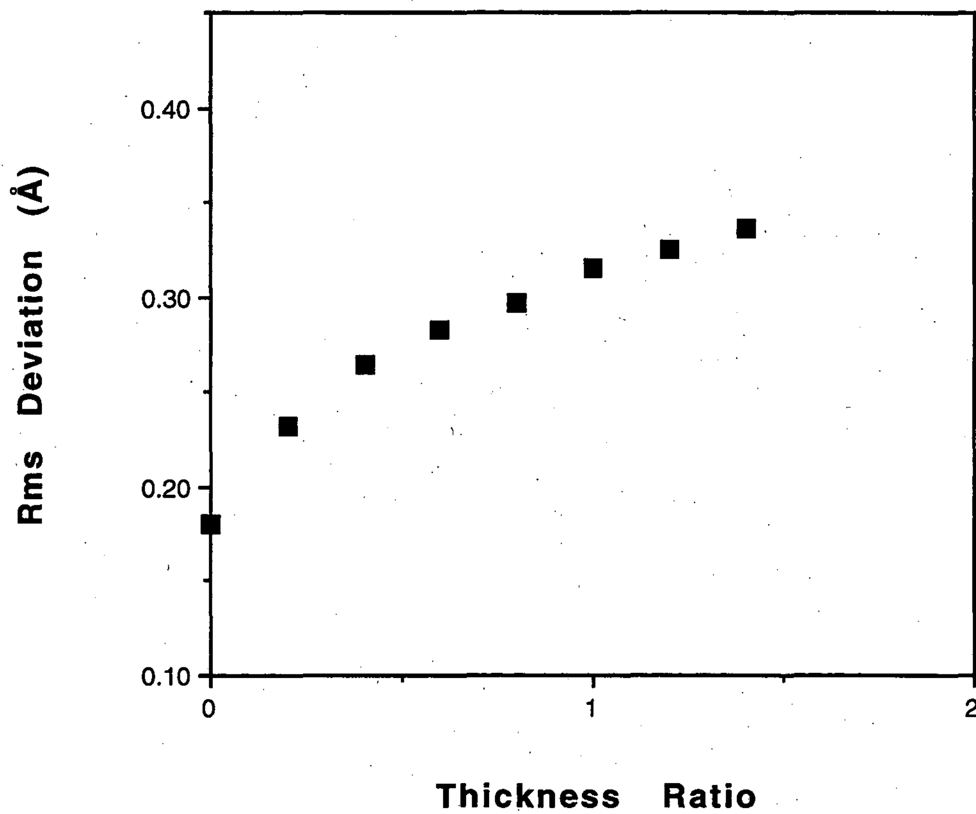

Figure 2a

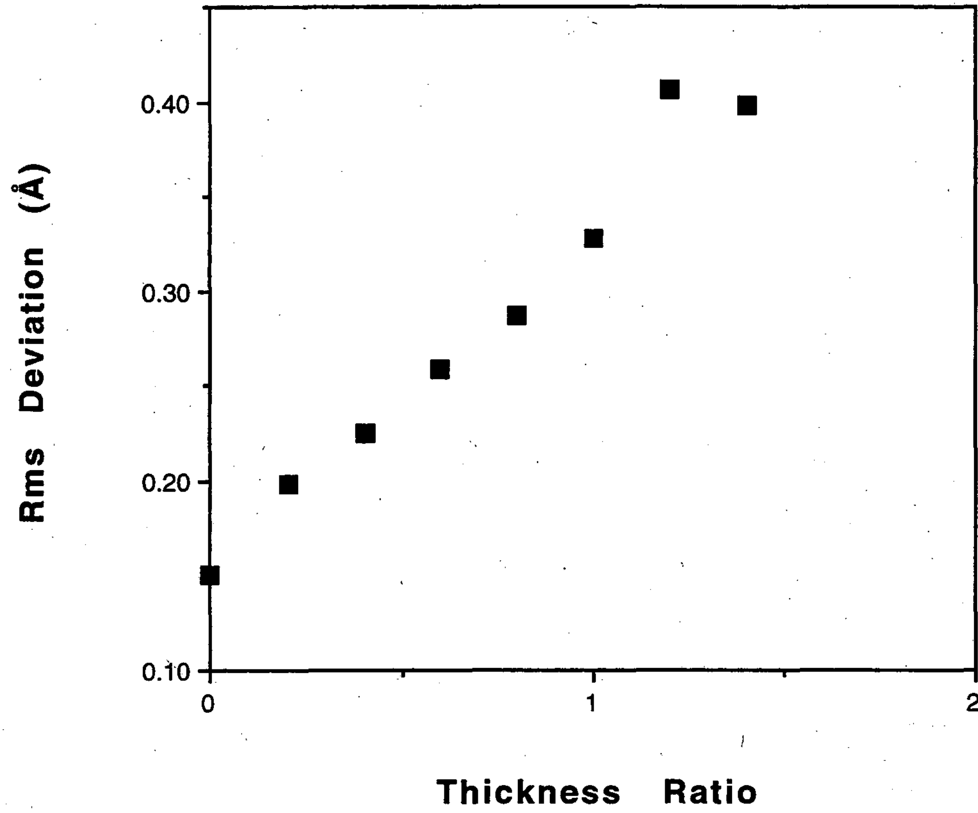

Figure 2b

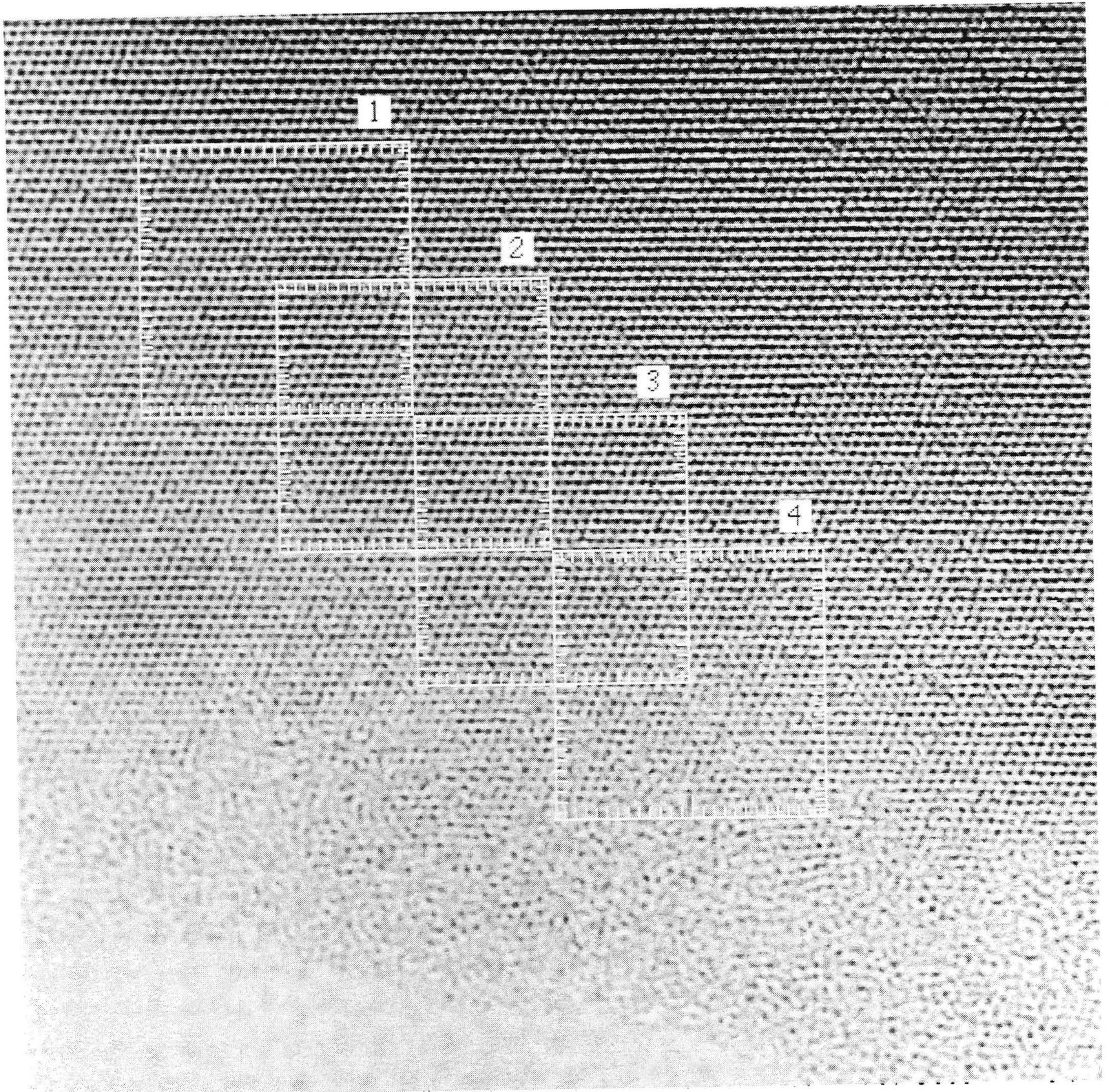

Figure 3

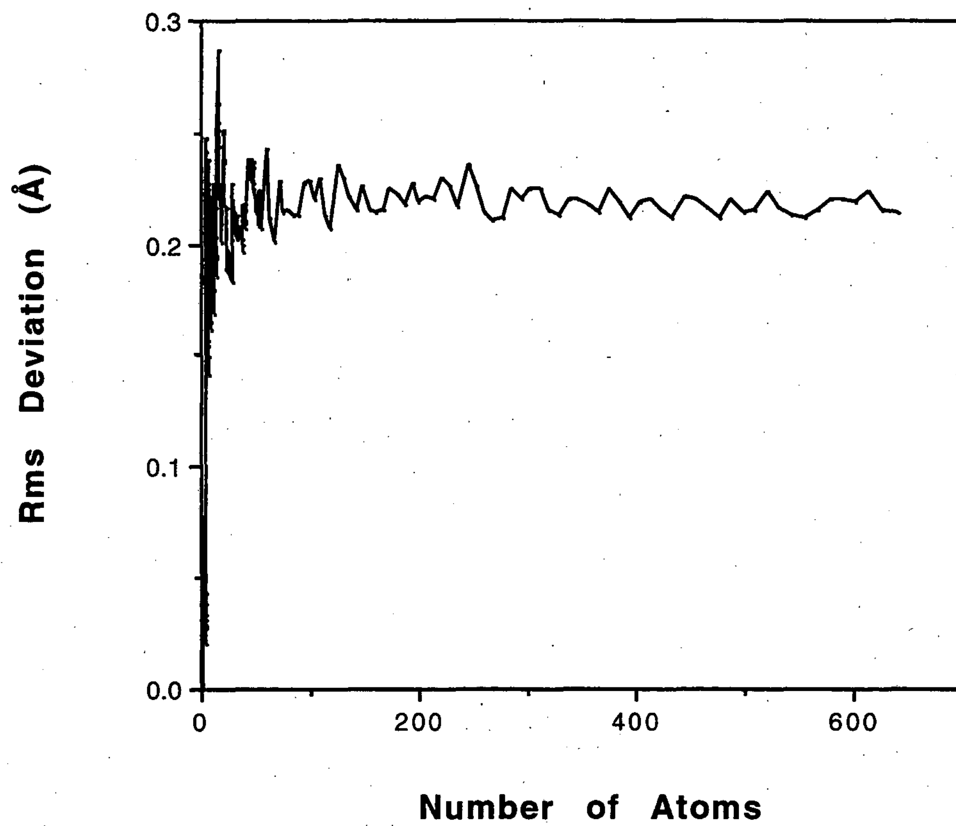

Figure 4a.

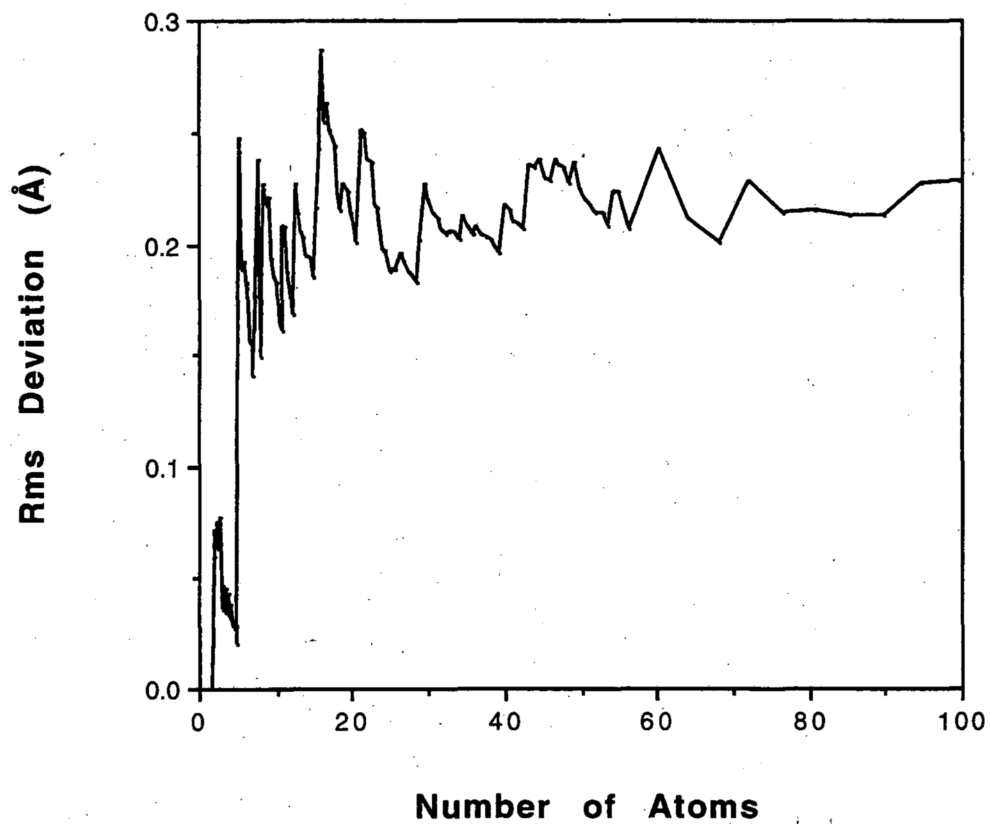

Figure 4b

LAWRENCE BERKELEY LABORATORY
UNIVERSITY OF CALIFORNIA
TECHNICAL INFORMATION DEPARTMENT
BERKELEY, CALIFORNIA 94720